Mecánica Computacional Vol. XXIII, pp. 59-78
G.Buscaglia, E.Dari, O.Zamonsky (Eds.)
Bariloche, Argentina, November 2004

THERMO-ELASTO-VISCOPLASTIC MODELING OF THE BEHAVIOR OF METALS SUBMITTED TO FINITE STRAINS. A COUPLED THERMO-MECHANICAL APPROACH.

Jean-Philippe Ponthot*and Laurent Adam†

*LTAS-Continuum Mechanics and Thermomechanics
University of Liège, 1 Chemin des Chevreuils, B52/3, B4000 Liège-1, Belgium.
e-mail : JP.Ponthot@ulg.ac.be , web page: http://www.ulg.ac.be/ltas-mct/
†LTAS-Continuum Mechanics and Thermomechanics
Currently at: e-Xstream engineering SA, 4 Av G. Lemaitre, B-1348 Louvain-la-Neuve, Belgium.
e-mail: laurent.adam@e-xstream.com , web page: http://www.e-Xstream.com

Key Words: Thermo-mechanical coupling, large strains, finite element, elasto-viscoplastic behavior, contact.

Abstract. *Our goal in this paper is to present a complete thermo-viscoplastic formulation at finite strains and its implementation into a finite element code. The formulation is derived from the classical J2-viscoplasticity with a flow criterion expressed in the current configuration in terms of the Cauchy stress tensor and the temperature distribution.*

A staggered scheme will be used for the resolution of the thermomechanical problem as well as an extension of the radial return algorithm for the integration of the constitutive law. Indeed,as Simo & Miehe showed,[1] staggered schemes are very attractive in comparison with monolithic (or simultaneous) schemes mainly because they involve the resolution of two linear symmetric systems in place of one larger nonsymmetric linear system.

In the next sections we will briefly formulate the fundamentals of the kinematics for a large deformation approach, and the basic equations governing our model.

After this, we will explain, in more details, the foundation of the staggered scheme and of the radial return algorithm introduced before.

We will also describe the basis of the methodology used to take into account thermomechanical frictional contact problems. The formulation is inspired by those of Johansson & Klarbring[2] and Oancea & Laursen.[3] The constitutive equations used to quantify the amount of heat exchange between two bodies in frictional contact being based on the work of Yovanovich.[4,5]

1 MATHEMATICAL FOUNDATION OF THE THERMO-VISCOPLASTIC MODEL AT FINITE STRAINS

1.1 Kinematics for large deformation continuum

Let us consider two configurations of a body : first, the reference configuration (not necessarily the initial configuration) at a certain time t_0 where the position of a material particle at this time is denoted by its *position vector* $\boldsymbol{X}$ and second, the current configuration, at time t, where the position of the same material particle is $\boldsymbol{x}$. Then there exists a mapping between $\boldsymbol{x}$ and $\boldsymbol{X}$ of the form

$$\boldsymbol{x} = \boldsymbol{x}(\boldsymbol{X}, t) \tag{1}$$

The *velocity* of the reference point $\boldsymbol{X}$ is the material time derivative of the position vector and is defined by

$$\boldsymbol{v} = \dot{\boldsymbol{x}} = \frac{\partial \boldsymbol{x}(\boldsymbol{X}, t)}{\partial t} \tag{2}$$

The *deformation gradient* of the motion at $\boldsymbol{X}$ is the second-rank two-point tensor $\boldsymbol{F}$ such that

$$\boldsymbol{F} = \frac{\partial \boldsymbol{x}}{\partial \boldsymbol{X}} \qquad \text{with} \qquad J = \det \boldsymbol{F} > 0 \tag{3}$$

By the polar decomposition, we can uniquely decompose $\boldsymbol{F}$ as

$$\boldsymbol{F} = \boldsymbol{R}\boldsymbol{U} \qquad \text{with} \qquad \boldsymbol{R}^{\mathrm{T}}\boldsymbol{R} = \boldsymbol{I} \qquad \text{and} \qquad \boldsymbol{U} = \boldsymbol{U}^{\mathrm{T}} \tag{4}$$

The corresponding *spatial gradient of velocity* is given by

$$\boldsymbol{L} = \frac{\partial \boldsymbol{v}}{\partial \boldsymbol{x}} = \dot{\boldsymbol{F}}\boldsymbol{F}^{-1} \tag{5}$$

It can be decomposed into the symmetric and the antisymmetric parts, $\boldsymbol{L} = \boldsymbol{D} + \boldsymbol{W}$ with

$$\boldsymbol{D} = \tfrac{1}{2}\left(\boldsymbol{L} + \boldsymbol{L}^{\mathrm{T}}\right) \qquad \text{the rate of deformation} \tag{6}$$

$$\boldsymbol{W} = \tfrac{1}{2}\left(\boldsymbol{L} - \boldsymbol{L}^{\mathrm{T}}\right) \qquad \text{the spin tensor} \tag{7}$$

1.2 Conservation equations

In this section, we will briefly formulate the fundamental set of conservation equations of a thermomechanical formulation.

1.2.1 Mechanical part

The equations used in this part of the formulation are the classical, and well known, conservation equations of the mass and of the momentum. Thus we won't write these in this section (see e.g. Malvern[6]).

1.2.2 Thermal part

The equation of heat is derived from the first principle of thermodynamics. We have decided, given a certain choice of state variables and a model for the description of the kinematics of the body, to express that equation as (see[1,7] for more details) :

$$\rho c_v \dot{T} - \dot{W}^{\text{thel}} + \rho \frac{\partial}{\partial \boldsymbol{\alpha}} [\psi - T \frac{\partial \psi}{\partial T}] . \dot{\boldsymbol{\alpha}} = \dot{W}^{\text{irr}} + \rho r - \text{div } \boldsymbol{q} \tag{8}$$

where ρ is the density, c_v is the specific heat at constant volume, T is the temperature, $\dot{W}^{\text{thel}}$ is the thermoelastic dissipation term, ψ is the Helmholtz's free energy, $\boldsymbol{\alpha}$ is the vector of internal state variables, $\dot{W}^{\text{irr}}$ is the viscoplastic dissipation term, r is the heat source and $\boldsymbol{q}$ is the thermal flux referring to the current configuration and linked to the temperature gradient by the well known Fourier's equation. Our choice of observable and internal state variables is $[\boldsymbol{\epsilon}^{\text{rev}}, T, \boldsymbol{\alpha}]$ where $\boldsymbol{\epsilon}^{\text{rev}}$ is a representative tensor of the reversible part of the deformation, thus $\psi(\boldsymbol{\epsilon}^{\text{rev}}, T, \boldsymbol{\alpha})$. In a further section we will describe in more details the two dissipation terms of this equation.

1.3 Constitutive equations

1.3.1 General formulation

It is generally assumed, see e.g. Whertheimer[8] and Wriggers et al.[9] for details, that the rate of deformation can be additively decomposed into an elastic (reversible), an inelastic (irreversible) and a thermal parts, i.e. $\boldsymbol{D} = \boldsymbol{D}^{\text{e}} + \boldsymbol{D}^{\text{vp}} + \boldsymbol{D}^{\text{th}}$ and that the hypoelastic stress-strain relation is given, for elasto-viscoplastic materials, by a relation of the type

$$\overset{\triangledown}{\sigma}_{ij} = H(T)_{ijkl}(D_{kl} - D^{\text{vp}}_{kl} - D^{\text{th}}_{kl}) \tag{9}$$

where $\boldsymbol{H}(T)$ is the Hooke stress-strain tensor at the temperature T given by

$$H(T)_{ijkl} = K(T)\ \delta_{ij}\delta_{kl} + 2G(T)\ (\delta_{ik}\delta_{jl} - \frac{1}{3}\delta_{ij}\delta_{kl}) \tag{10}$$

in which

$\overset{\triangledown}{\boldsymbol{\sigma}}$	is an objective rate of Cauchy stress tensor,
$\boldsymbol{D}$	is the rate of deformation,
$\boldsymbol{D}^{\text{vp}}$	is the viscoplastic part of $\boldsymbol{D}$,
$\boldsymbol{D}^{\text{e}}$	is the elastic part of $\boldsymbol{D}$,
$\boldsymbol{D}^{\text{th}}$	is the thermal part of $\boldsymbol{D}$,
$\boldsymbol{\delta}$	is the Kronecker delta symbol
$K(T)$	is the bulk modulus of the material at T
$G(T)$	is the shear modulus of the material at T

Classically, for a $J2$ von Mises material with isotropic hardening, we assume the existence of a *yield function* f given by

$$f(\boldsymbol{\sigma}, \sigma^v, T) = \bar{\sigma} - \sigma^v(T) = 0 \tag{11}$$

where
- $\bar{\sigma}$ is the effective stress, i.e. $\bar{\sigma} = \sqrt{\frac{3}{2}\boldsymbol{s} : \boldsymbol{s}}$;
- $\boldsymbol{s}$ is the deviator of the stress tensor;
- $\sigma^v(T)$ is the current yield stress.

With this approach, the admissible stress states are constrained to remain on or within the elastic domain ($f \leq 0$).

In this elasto-viscoplastic formulation, the effective stress $\bar{\sigma}$ is no longer constrained to remain less or equal to the yield stress but one can have $\bar{\sigma} \geq \sigma^v(T)$. Therefore we define the *overstress* as

$$d = \langle \bar{\sigma} - \sigma^v(T) \rangle \tag{12}$$

where $\langle x \rangle$ denotes the Mac Auley brackets defined by $\langle x \rangle = 1/2(x + |x|)$. Clearly, an inelastic process can only take place if, and only if, the overstress d is positive. In that case, $f \geq 0$.

The notion of irreversibility, linked to the viscoplastic part, is built into the formulation by introducing nonsmooth equations of evolution for $\boldsymbol{D}^{\text{vp}}$ (flow rule) and $\sigma^v(T)$ (hardening laws) as follows.

1.3.2 Flow rule

When viscoplastic deformation occurs, $f \geq 0$ and one can write, in the case of associative viscoplasticity:

$$\boldsymbol{D}^{\text{vp}} = \Lambda \boldsymbol{N} \qquad \text{where} \qquad \boldsymbol{N} = \frac{\partial_\sigma f}{\|\partial_\sigma f\|} \tag{13}$$

is the unit outward normal ($\boldsymbol{N} : \boldsymbol{N} = 1$) to the yield surface and Λ is a positive parameter called the *consistency parameter*. In a viscoplastic formulation, Λ cannot be determined, as in J2-plasticity, by expressing the so-called consistency condition.

So one more equation is needed to be able to express that consistency parameter, and so on the viscoplastic part of the rate of deformation. Various model were proposed to express Λ in terms of the current stress level. For example, classical viscoplastic models of the Perzyna type[10,11] use a consistency parameter of the form :

$$\Lambda = \sqrt{\frac{3}{2}} \left\langle \frac{\bar{\sigma} - \sigma^v(T)}{\eta(\bar{\epsilon}^{\text{vp}}, T)^{1/n(T)}} \right\rangle^{m(T)} \tag{14}$$

where
- $n(T)$ is a hardening exponent
- $m(T)$ is a rate sensitivity parameter
- $\eta(T)$ is a viscosity parameter.

This consideration can be viewed as a penalty regularization of rate-independent plasticity ($f \leq 0$) where the consistency parameter has been replaced by an increasing function of the overstress.

1.3.3 Isotropic hardening law

The evolution equation of the internal variable σ^v (which, in this case, is the only internal variable) is given by:

$$\dot{\sigma^v} = \sqrt{\frac{2}{3}}\, h(T)\, \Lambda \tag{15}$$

with $h(T)$ is called the *plastic modulus* and corresponds to the slope of the effective stress vs. effective plastic strain curve under uniaxial loading conditions. Generally, h is a function of the effective viscoplastic strain, leading to a non-linear evolution equation for σ^v. Equation (15) can also be rewritten, in this more general case, as

$$\dot{\sigma^v} = h(T, \bar{\epsilon}^{\mathrm{vp}})\, \dot{\bar{\epsilon}}^{\mathrm{vp}} \tag{16}$$

where $\dot{\bar{\epsilon}}^{\mathrm{vp}}$ is the rate of effective viscoplastic strain defined as

$$\dot{\bar{\epsilon}}^{\mathrm{vp}} = \sqrt{\frac{2}{3}\boldsymbol{D}^{\mathrm{vp}} : \boldsymbol{D}^{\mathrm{vp}}} = \sqrt{\frac{2}{3}}\Lambda = \left\langle \frac{\bar{\sigma} - \sigma^v(T)}{\eta(\bar{\epsilon}^{\mathrm{vp}}, T)^{1/n(T)}} \right\rangle^{m(T)} \tag{17}$$

so that, in the viscoplastic range, one can define a new constraint

$$\bar{f} = \bar{\sigma} - \sigma^v(T) - \eta(\bar{\epsilon}^{\mathrm{vp}}, T)^{1/n(T)} (\dot{\bar{\epsilon}}^{\mathrm{vp}})^{1/m(T)} = 0 \tag{18}$$

This criterion is a generalization of the classical von-Mises criterion $f = 0$ for rate-dependent materials. The latter can simply be recovered by imposing $\eta = 0$ (no viscosity effect).

1.3.4 Thermal Part

The equation governing the evolution of the thermal part of the tensor of the rate of deformation is a generalization of the equation used in infinitesimal strain theory, which is given by :

$$D_{ij}^{\mathrm{th}} = \beta\, \dot{T}\, \delta_{ij} \tag{19}$$

where β is the linear thermal expansion coefficient.

1.4 Discussion of the dissipation terms of the heat equation

1.4.1 Viscoplastic heating

The viscoplastic heating $\dot{W}^{\mathrm{irr}}$, as introduced above, is the most important heating source due to a mechanical deformation. As explained in[1] a part of the viscoplastic deformation does not create heat but induces the stocking of energy in the materials through the creation of micro-stress fields linked to the development of dislocations and another microscopic defects. That part of non recoverable energy is expressed by the term :

$$\rho \frac{\partial}{\partial \boldsymbol{\alpha}} [\psi - T \frac{\partial \psi}{\partial T}]\, \dot{\boldsymbol{\alpha}} \tag{20}$$

in equation (8). This term is usually managed in considering that it represent, in the area of metal forming, between 5% and 15% of $\dot{W}^{\text{irr}}$. So, these two terms merge in a unique expression written as $\chi \dot{W}^{\text{irr}}$ where χ is a multiplicative factor which classically takes its value between 0.85 and 0.95.

Considering the flow rule introduced before we can express the viscoplastic heating as :

$$\dot{W}^{\text{irr}} = \bar{\sigma}\, \dot{\bar{\epsilon}}^{\text{vp}} \tag{21}$$

1.4.2 Thermoelastic heating

The thermoelastic heating, represented by the term $\dot{W}^{\text{thel}}$ in equation (8), has a minor contribution to the thermal equation. Many authors have neglected this term but, as a precise analyse can show, it has a stabilizing effect on the solution schemes used in the field of thermo-elasto-viscoplastic problem.

It can be expressed, using some properties of the viscoplastic flow, as :

$$\dot{W}^{\text{thel}} = 3K(T)\beta T \frac{\dot{J}}{J} \tag{22}$$

2 INTEGRATION PROCEDURE

In this section we will briefly describe the main steps of numerical schemes able to solve these equations in time :

2.1 Formulation of the problem to solve

Let us consider $[t_n, t_{n+1}]$ a sub-interval of the global time interval of interest, and ϕ the vector of primary variables defined as :

$$\phi = (\boldsymbol{x}, \boldsymbol{v}, T) \tag{23}$$

To determine ϕ at the time t_{n+1} we need to integrate the constitutive law, using the value of the internal variables $\boldsymbol{\alpha}$ at t_n, to evaluate $\boldsymbol{\alpha}$ at t_{n+1}. This part of the integration procedure will be described in section 3.3 .

The problem under consideration can be formulated as a first order problem of evolution written as :

$$\dot{\boldsymbol{x}} = \boldsymbol{v} \tag{24}$$

$$\dot{\boldsymbol{v}} = \frac{\text{div}\boldsymbol{\sigma}}{\rho} + \boldsymbol{b} \tag{25}$$

$$\dot{T} = \frac{1}{\rho c_v}[\rho r - \text{div}\boldsymbol{q} + \dot{\text{W}}^{\text{irr}} + \dot{\text{W}}^{\text{thel}}] \tag{26}$$

in the interval $[t_n, t_{n+1}]$ and on the whole body.

2.2 Staggered schemes

In our model we have decided to use the backward-Euler formula for the approximation of the time derivative, and the finite element technique for the spatial discretization. Under above assumptions it's easy to show that a monolithic scheme, if applied to this problem, will induce the resolution of a linear unsymmetrical system of order $(n_{\mathrm{dim}}+1).n_{\mathrm{node}}$, where n_{dim} is the dimension of the space and n_{node} is the number of node of the finite element mesh. Staggered schemes, based on a split of the operator defined by the equations (24, 25, 26), have been developed to reduce the computational cost of such resolution.

2.2.1 Isothermal split :

The simplest split consists in the decomposition of the global thermomechanical operator in a mechanical operator at fixed temperature and a thermal operator at fixed geometry. This split leads to the resolution of two symmetric linear systems, the first of order $n_{\mathrm{dim}}.n_{\mathrm{node}}$ and the second of order n_{node} involving respectively the two equations (24, 25) and the equation (26). This scheme of resolution results only in a conditional stability which can be improved by the modification introduced by Armero & Simo[12] and described below.

2.2.2 Adiabatic split :

This split consists in the decomposition of the global thermomechanical operator in a mechanical operator at fixed entropy and a thermal operator at fixed geometry. This modification consists in the resolution of one part of the equation (26) during the first phase to transform that phase into an adiabatic one. That part of the equation can be solved analytically, a fact that enables us to keep the same order for the linear systems of both phases.

2.3 The radial return mapping algorithm

For a given configuration defined by its known set of positions $\boldsymbol{x}(t_n)$ at time t_n the problem is now to update all state variables to a new configuration defined by its set of position $\boldsymbol{x}(t_{n+1})$ (which are supposed to be known) at time t_{n+1}. These incremental motions are, in turn, used to calculate the incremental strain history by means of the kinematic relations.

The problem dealt with in this paragraph is, for the given incremental strain history, to find the new values of the variables $(\boldsymbol{\sigma}_{\mathrm{n+1}}, \bar{\epsilon}^{\mathrm{vp}}_{n+1}, \sigma^{v}_{n+1})$ at t_{n+1}. These are obtained by integration of the local constitutive equations with initial conditions given by $(\boldsymbol{\sigma}_{\mathrm{n}}, \bar{\epsilon}^{\mathrm{vp}}_{n}, \sigma^{v}_{n})$ at t_n. To integrate these equations in time, we will rely on the general methodology of elastic-predictor /plastic-corrector (return mapping algorithm), as synthesized by Simo & Hughes[13] but here, we will extend this methodology to the time-dependent case.

In a first step, the elastic predictor problem is solved with initial conditions that are the converged values of the previous time step while keeping irreversible variables frozen. This produce a trial elastic stress state $\boldsymbol{\sigma}_{\mathrm{tr}}$ which, if outside the yield surface f is taken as the initial conditions for the solution of the viscoplastic corrector problem. The objective of this second

step is to restore consistency by returning back the trial stress to the generalized criterion $\bar{f}$ (and not on the yield function f as is done in the rate-independent case!). For more details about this algorithm see Ponthot.[14]

3 MATHEMATICAL FOUNDATION OF THE THERMOMECHANICAL FRICTIONAL CONTACT PROBLEM

3.1 Introduction

In this section the problem to be solved deals with the computation of the mechanical and thermal forces generated by contact interactions between two flexible bodies. Our goal is not to develop entirely the methodology used to tackle this type of problem (the authors address the interested reader to references[15] and[16]) but to expose briefly its basis and to describe in more details thermal aspects.

In what follows we will use the finite element method to spatially discretize the body under consideration. As explained in[15] quadrilateral or hexahedral linear elements (with constant pressure) is, in the field of large deformation analysis, a good choice in order to develop an accurate finite element code. Thus, in this section, we will focus on linear contact elements and on the penalty method that we use to impose the non penetration condition. We also use a node to segment approach such that a typical contact finite element is composed of a "slave" node and a "master" segment.

General methodology

A typical contact finite element is represented in figure 1. Assuming this type of geometry we can define a penetration $g_N \geq 0$ which is the minimal distance between the slave node $\mathbf{x}$ and its closest projection on the master segment $\mathbf{x_p}$. From this definition of the penetration we compute

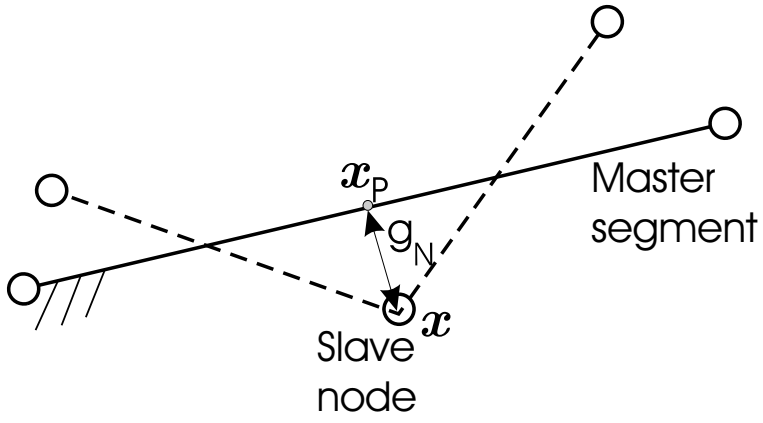

Figure 1: Topology of a contact element

the normal contact force using the penalty method. We obtain :

$$t_N = c_N \, g_N \tag{27}$$

where t_N is the normal contact force and c_N the normal penalty parameter. We also have to compute the reaction to this contact force, which is subsequently distributed with respect to the relative tangential position of $\mathbf{x_p}$ over the two master nodes, which act on the master segment.

In the same way, if we define properly a sliding distance of the slave node over the master segment $g_T \geq 0$ we can define tangential contact forces which are evaluated as follows :

$$|\boldsymbol{t_T}| = c_T\, g_T\, if\; c_T\, g_T \leq \mu_{sta} t_N (sticking) \tag{28}$$

$$|\boldsymbol{t_T}| = \mu_{dyn}\, t_N\, if\; c_T\, g_T \geq \mu_{sta} t_N (sliding) \tag{29}$$

where μ_{sta} and μ_{dyn} are respectively the static and dynamic coefficient of friction, $|\boldsymbol{t_T}|$ is the modulus of the tangential contact forces vector (its direction being the opposite of the sliding direction) and c_T the tangential penalty parameter. Note that the coefficients of friction μ_{sta} and μ_{dyn} don't vary with temperature changes. This type of dependency is quite difficult to model and no general law describing these variations is available. For this reason the authors will omit this aspect here.

Concerning the computation of the mechanical forces, each node which is susceptible to get into contact is successively considered as a slave node (all the other nodes describing master surfaces) and as defining, with another nodes, a master surface.

For the computation of the thermal fluxes generated during contact conditions we also need to allot a characteristic area A to the slave node. Some authors use the area of the master segment as a characteristic area, others use the neighbors of the slave node to define a surface. In this paper we will follow the second type of approach because of the following arguments : If two slaves nodes are in contact with the same master segment, and if we want to use the surface of this segment to evaluate the contact area, we are forced to divide the length of the master segment and to assign a part to each slave node. So, for example, the total heat transferred between the bodies through the first slave node depends on whether or not the second slave node is in contact. If we choose not to divide the master segment the heat exchange between the master segment and the part of the slave body which is in contact will depend on the number of nodes which discretize the slave body. For these reasons we choose to evaluate the characteristic area associated to a contact node from the geometry of the two segments formed by the slave node and its first two neighbors. Compared with classical methods, we use a slightly different way to evaluate this area (see left figure 2) as we suppose that it is equal to $(L_1 + L_2)/2$ (usually it is equal to $(L_1^* + L_2^*)/2$). This choice is consistent with the best method to evaluate the contact pressure from the external contact forces. It seems also more correct to us as it takes into account the local geometry of the slave surface to define correctly an heat flux. Of course, as illustrated on the right side of figure 2, if L_1 or L_2 become negative, its value is fixed to zero.

3.2 Thermal aspects of the frictional contact problem

Computing the thermal fluxes and dissipations during the contact between two bodies, we extend here mechanical contact interactions to thermomechanical contact interactions.

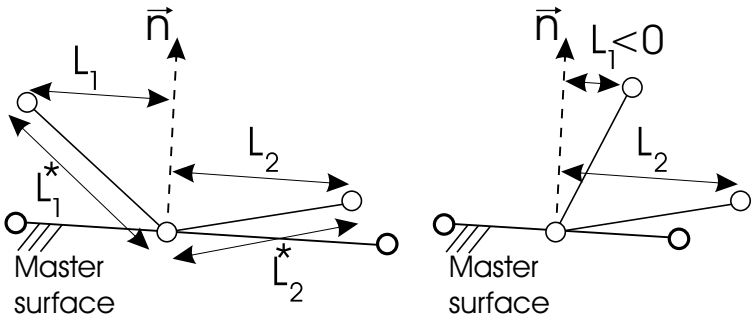

Figure 2: Evaluation the contact area

The expression used for the thermal fluxes and dissipation are respectively :

$$Q = q_c A = (q_i.n_i)A = h(T_{sla} - T_{mas})A \tag{30}$$

$$D_{tot} = D_{sla} + D_{mas} = |\boldsymbol{F_T}|\ \dot{g_T} \tag{31}$$

$$with\ D_{sla} = \eta^r_{sla} D_{tot} \tag{32}$$

$$D_{mas} = \eta^r_{mas} D_{tot} \tag{33}$$

where Q is the heat exchange between the two bodies, q_c is the corresponding heat flux, q_i is i^{th} component of that heat flux vector, n_i is the i^{th} component of the unit normal defined at $\mathbf{x_p}$, h is the contact heat transfer coefficient, T_{sla} is the temperature of the slave node, T_{mas} is the temperature at $\mathbf{x_p}$, D_{tot} is the total dissipation, D_{sla} and D_{mas} are respectively the part of the dissipation which is assigned to the slave node and to the master segment, η^r_{sla} and η^r_{mas} are the relative effusivity of the slave node and of the master surface, $\boldsymbol{F_T}$ is the total tangential contact force vector (adding contribution $\boldsymbol{t_T}$ as a slave node and contact reactions as a node of a master surface) acting on the slave node, and $\dot{g_T}$ is the sliding velocity of the slave node over the master segment (which is evaluated using the assumption of linear evolution of g_T between the current and the reference configurations).

In the same way as for the mechanical forces, we have to compute the thermal reaction corresponding to Q over the master segment. However, concerning the thermal forces computation, each node will only be considered as a slave node or defining a master surface.

We have to note that if the node is sticking, even if it is possible to define a reversible sliding distance, and so on a sliding velocity, we set D_{tot} at zero.

Concerning the contact heat transfer coefficient we will use a simple model (but also very accurate and well known) which is a simplification of the more complex models exposed in the references.[4,5] This model expresses the thermal heat transfer coefficient as[4] :

$$h = h_0(\frac{p}{H})^e \tag{34}$$

where h_0 is a nominal heat transfer coefficient, p is the contact pressure, H is the Vickers hardness and e is an exponent which takes a value between 0.8 and 1.

4 NUMERICAL APPLICATIONS

4.1 Forming of a quarter cylinder.

This numerical test has, especially, the aim of showing the importance of the thermal spring-back, and so of the unloading phase, at different forming temperatures. The material parameters are typical for an aluminium alloy which has a superplastic behavior at high temperature.

The test conditions are represented in the Figure 3. The right end of the sheet is clamped and the die has a fixed position. The pressure and the temperature are, in a first phase, increased to their forming values, then they are maintained during the forming of the sheet, and finally lowered to their room values. In the results exposed below, the thickness to die radius ratio is $\frac{1}{50\pi}$. The forming time is 3100s (300s for the loading, 2700s for the stress relaxation and 100s for the unloading).

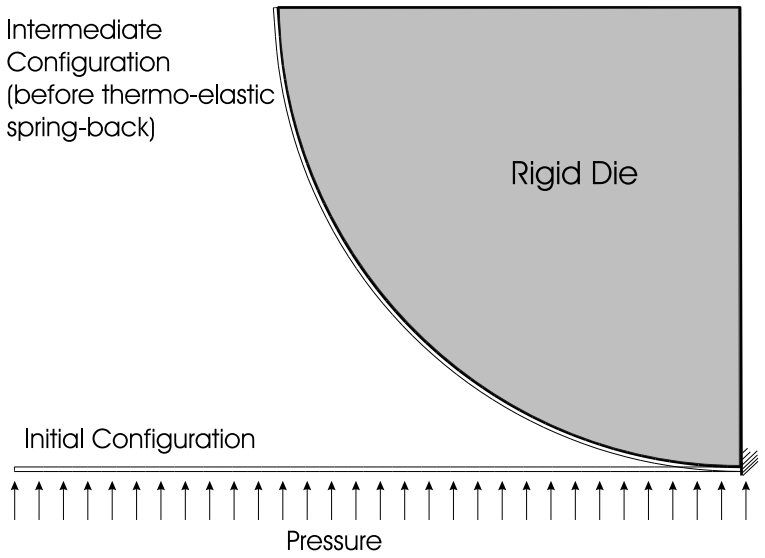

Figure 3: Description of the process setup

Figure 4 shows final configurations for the different forming temperatures. We observe that the cold forming of the sheet induce few irreversible deformations and so the spring-back is almost total. On the other hand, for the forming at high temperature, there is almost no spring back. The final stress level is a decreasing function of the forming temperature, as we can see in the next two Figures (Figures 5 and 6). These stress distributions are plotted in the initial configuration with a dilatation factor of 15 along the vertical axis.

4.2 Frictional heating between two blocks

In this example we will study the mechanism of heating due to frictional sliding. We consider here the relative sliding of two deformable blocks (figure 7) which are able to conduct heat. This numerical example was used by Wriggers & Miehe[17] and also by Agelet de Saracibar[18] (with a pseudo-3D formulation) to validate their models. In their approach these authors consider

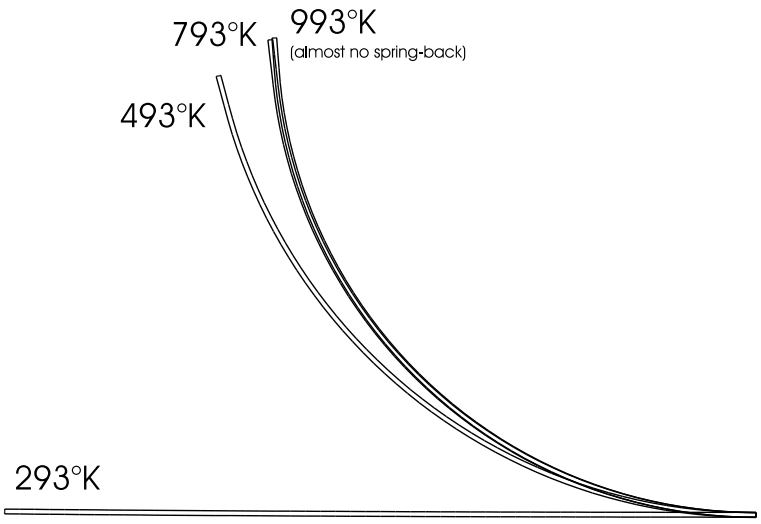

Figure 4: Final configurations for different forming temperatures

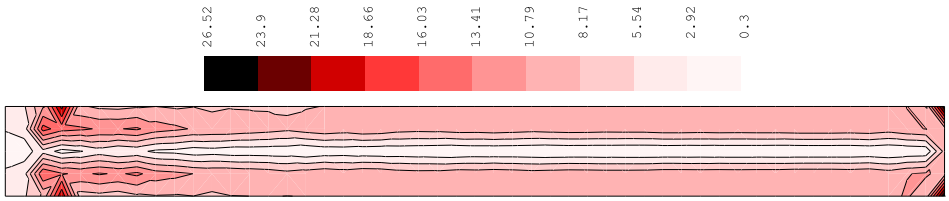

Figure 5: Final distribution of the J2 stress in MPa (forming at 493°K)

that the lower block is rigid which is not the case in the present test. As the contact pressure is relatively low, and thus the level of deformation, this difference has negligible effects on the solution.

The upper block is driven via its upper face and the total displacement ($3.75mm$) is applied within $3.75\ 10^{-3}s$. A pressure of $10N/mm^2$ is also applied to keep the two blocks in contact and a frictional coefficient of 0.2 is used.

The discretization uses 10x10 linear elements for the upper block and 30x10 elements for the lower one. The mechanical boundary conditions are shown in figure 7. The two blocks are considered to be thermally isolated from their environment and the thermal heat flux exchanged between the two bodies and the frictional dissipation term are computed as described in section

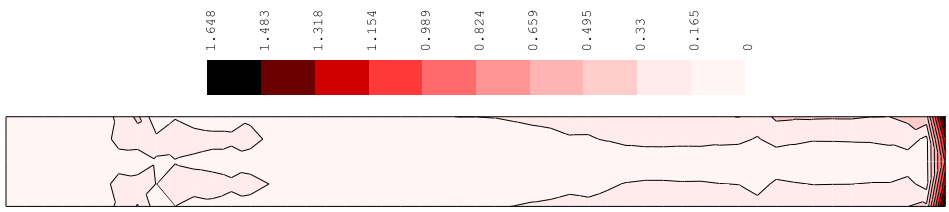

Figure 6: Final distribution of the J2 stress in MPa (forming at 993°K)

3. An elasto-plastic constitutive law is used with linear isotropic hardening. The material parameters are the same for the two blocks and are given in the table 1 for the continuum and in the table 2 for the surface. The initial (and reference) temperature is $300K$ and penalty parameters for the contact problem are taken as $c_N = c_T = 10^3\ N/mm$. An isothermal split is used to resolve the quasi-static thermomechanical problem.

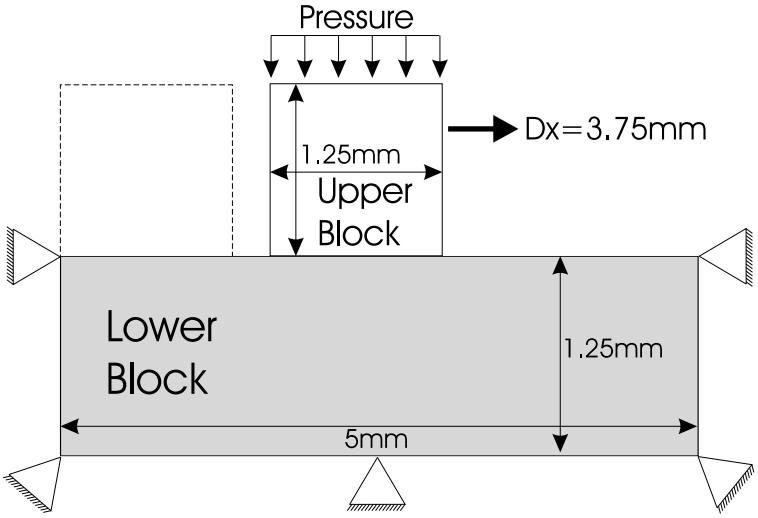

Figure 7: Frictional heating between two blocks : Description

Bulk modulus	$70000N/mm^2$
Poisson's ratio	0.3
Initial yield stress	$150N/mm^2$
Linear hardening modulus	$50N/mm^2$
Density	$2.7\ 10^{-9}Ns^2/mm^4$
Thermal expansion coefficient	$23.86\ 10^{-6}K^{-1}$
Conductivity	$150N/sK$
Thermal capacity	$0.9\ 10^9mm^2/s^2K$

Table 1: Material parameters for the continuum

The temperature distribution at time $t = 3.10^{-3}s$ is shown in figure 8. It agrees quite well with those obtained by Agelet de Saracibar[18] and Wriggers & Miehe.[19] It is also possible to compare the numerical solution with an analytical result if, after $t = 3.75\ 10^{-3}s$, we stop the thermal exchanges between the two bodies and compute the thermal field up to an homogeneous temperature. This comparison is made in table 3.

Computational features of this numerical simulation are given in table 4.

Nominal heat transfer coeff.	$150 N/sK$
Vickers hardness	$932 Mpa$
Exponent e	0.95
Relative effusivity	0.5

Table 2: Material parameters for the surface

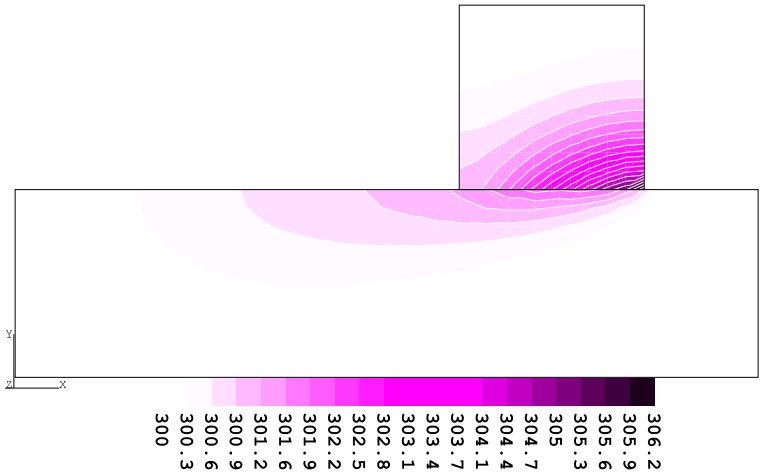

Figure 8: Temperature distribution (K) at $t = 3.10^{-3} s$

	Numerical	Analytical
Upper block	1.231 K	1.234 K
Lower block	0.307 K	0.308 K

Table 3: Final homogeneous temperature elevation : Numerical and analytical results

CPU	18.33 sec
Number of time steps	77
Number of iterations	217

Table 4: Computational features of the frictional heating between two blocks

4.3 Impact of cylindrical tube

This problem was studied by Beltran & Goicolea[20] (quasi-static formulation), by Garcia-Garino[21] (explicit dynamic formulation) and by Ponthot[15] (implicit dynamic formulation). This test has the aim to simulate the impact of a tube which occurs during a car crash. This type of tube is used to dissipate energy during the crash, in the form of plastic work. In this simulation we will show the importance of the thermal effects (in the bulk of the tube and on its surface) on the capability of the tube to resist to a force.

Due to the geometry (figure 9) we use axisymmetric finite elements to discretize the tube (6x200 elements) and assume the impacted base to be rigid. The computation is carried out using a dynamic implicit formulation with a generalized mid-point scheme.[15]

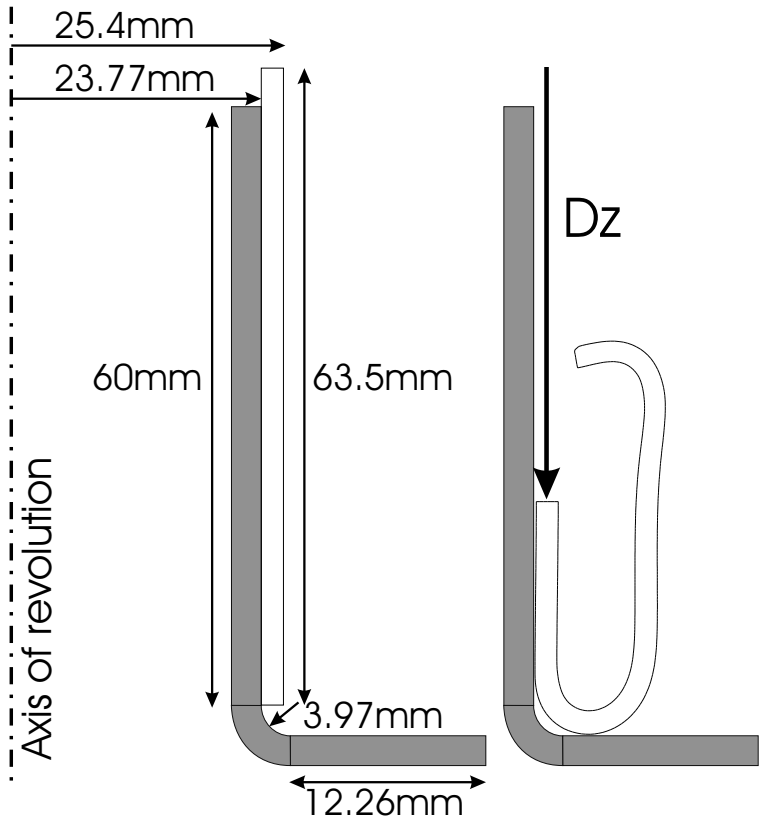

Figure 9: Initial and deformed geometries

We will study this application with an impact velocity of $55km/h$. As the cylinder is driven by its upper basis to a total vertical displacement Dz of $50mm$ the impact will last $3.27\ 10^{-3}s$.

Concerning the constitutive laws (for the continuum and the surface) we use the same approach as in the previous test (see tables 1 and 2) with a frictional coefficient of 0.08. Penalty parameters of $c_N = 10^5$ and $c_T = 10^4 N/mm$ are used and reference temperature is fixed at $293K$. An additional material parameter is introduced into the model to simulate the thermal

softening of the yield limit. The evolution law is thus given by :

$$\sigma_0^v(T) = \sigma_0^v(T_{ref})(1 - \omega_0(T - T_{ref})) \tag{35}$$

where σ_0^v is the initial yield limit, and ω_0 is the linear softening parameter. In this test ω_0 is set at $2.10^{-3}K^{-1}$.

Three different simulations were conducted (called case 1 to 3), respectively involving a purely mechanical formulation, a thermomechanical formulation without computation of the frictional heating and a thermomechanical formulation with computation of the frictional heating.

Figure 10 illustrates the final temperature distribution for cases 2 and 3. We can note that the temperature elevation along the inner skin of the tube is clearly more important if frictional dissipation is taken into account but is very localized. This localization of the "frictional heat affected zone" enables the cylinder to conserve its constitutive parameters, as the yield limit, unchanged. Thus, the required force to drive the vertical displacement is still the same in case 2 and 3.

The evolution of this force, for case 1 and 2, is illustrated in figure 11. Note that temperature elevation produced by the plastic work is approximately independent of the impact velocity because an elasto-plastic model has been used and not a viscoplastic one. From a physical point of view, frictional heating surely affects the coefficient of friction but we don't take into account this dependence.

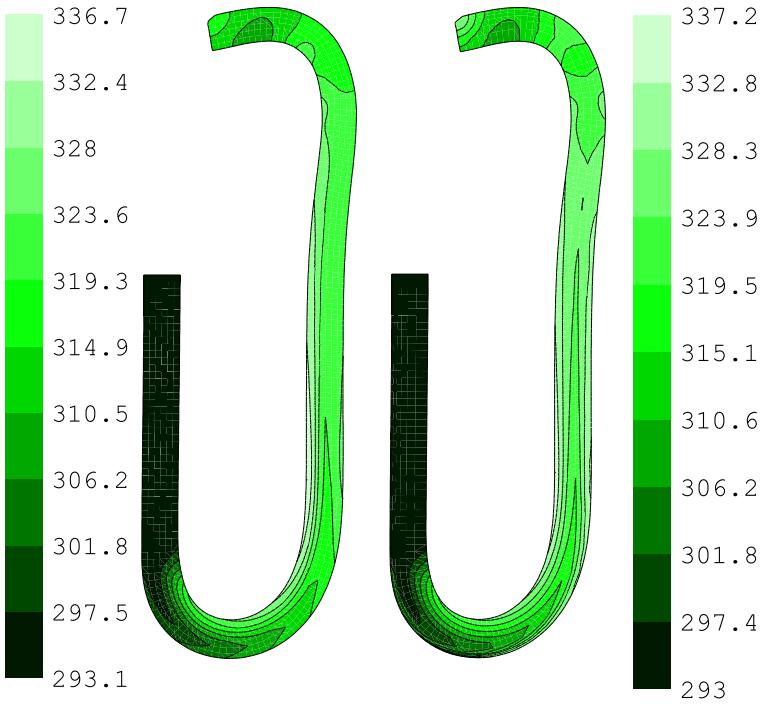

Figure 10: Final temperature distribution (K) : Without (left) and with (right) frictional heating (55 km/h impact)

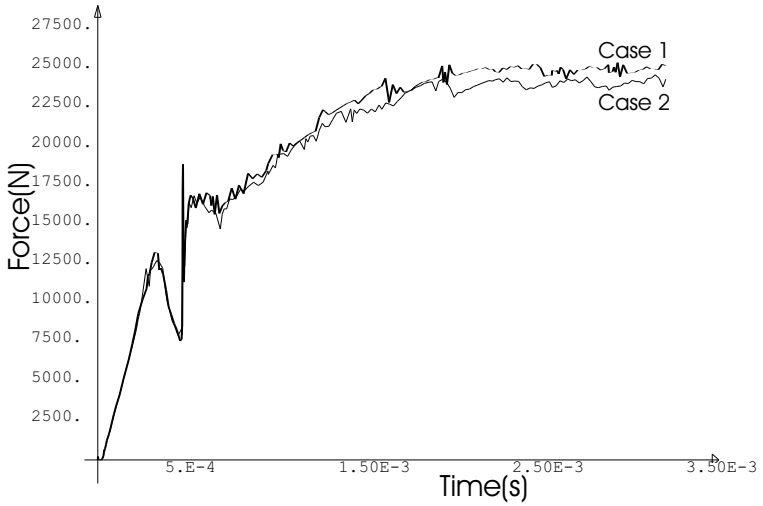

Figure 11: Evolution of the required force to drive the vertical displacement (55 km/h impact)
Case 1 : Purely mechanical analysis
Case 2 : Thermomechanical analysis without frictional heating

We can conclude that in this case of a fast process, the main influence of the frictional heating is probably the reduction of the coefficient of friction induced by the important softening of the surface asperities. This effect is not simulated and so the results are only indicative of the global behavior of the cylinder.

Figure 12 shows that the temperature elevation at point P is very important at the beginning of the process, because during that phase the vertical applied force acts only over a small area around point P inducing important frictional forces and heating.

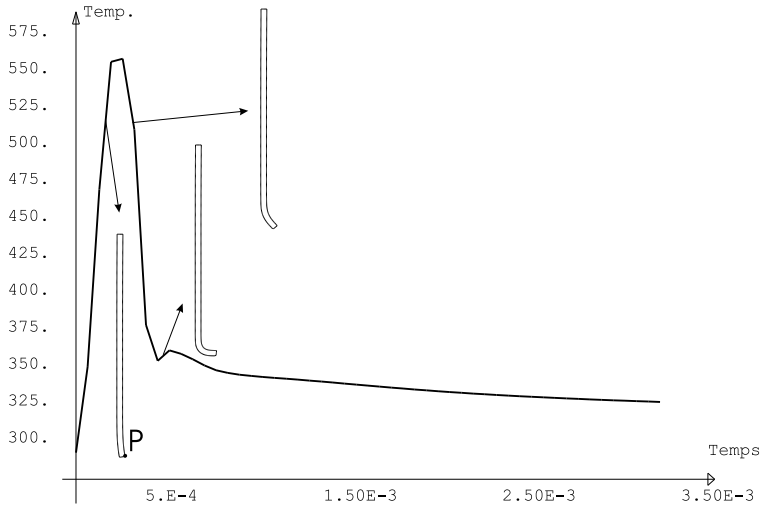

Figure 12: Temperature evolution at material point P (55km/h impact)

In the case of a thermomechanical analysis with evaluation of the frictional heating, this com-

putation involves 199 time steps and 755 iterations (199 thermal iteration and 556 mechanical iteration) leading to a CPU time of 4 min 11 s.

5 CONCLUSIONS

A complete thermo-elasto-viscoplastic framework was presented with the derived thermo-contact formulation. This formulation is able to simulate non-isothermal metal forming and impact processes.

Concerning contact interactions, a simple computational method was established which enables us to take into account temperature elevation induced by frictional sliding. Through these numerical simulations, we showed the influence of thermal softening, viscoplastic heating and frictional heating on the mechanical behavior of solids during their forming.

The unified way used to treat behaviors extending from elasticity to thermo-elasto-viscoplasticity at the Gauss point level and the isothermal staggered scheme, enables us to model entire metal forming processes composed of isothermal and anisothermal phases with large temperature changes in a unique simulation.

In the continuation of our research work, we will take into account temperature dependent coefficient of friction and more complex contact heat transfer models. These advances will enable us to simulate more precisely and completely crash or metal forming operations.

REFERENCES

[1] J.C. Simo and C. Miehe. Associative coupled thermoplasticity at finite strains formulation, numerical analysis and implementation. *Computer Methods in Applied Mechanics and Engineering*, **98**, 41–104 (1992).

[2] L. Johansson and A. Klarbring. Thermoelastic frictional contact problems : Modelling, finite element approximation and numerical realization. *Computer Methods in Applied Mechanics and Engineering*, **105**, 181–210 (1993).

[3] V.G. Oancea and T.A. Laursen. A finite element formulation of thermomechanical rate dependent frictional sliding. *International Journal of Numerical Methods in Engineering*, **40**, 4275–4311 (1997).

[4] S. Song and M.M. Yovanovich. Relative contact pressure : Dependence upon surface roughness parameters and vickers microhardness coefficicents. *Journal of Thermophysics and Heat Transfer*, **2**(1), 43–47 (1987).

[5] M.M. Yovanovich. Thermal contact correlations. *Progress in Astronautics and Aeronautics : Spacecraft Radiative Transfer and Temperature Control*, **83**, 83–95 (1981). T-E. Houston, ed.

[6] L.E. Malvern. *Introduction to the Mechanics of Continuous Medium*. Prentice-Hall, (1969).

[7] D. Rozenwald. *Modélisation thermomécanique des grandes déformations. Application aux problèmes de mise à forme des métaux, des élastomères et des structures mixtes métal-elastomère.* PhD thesis, University of Liège, Liège, Belgium, (1996).

[8] T.B. Whertheimer. Thermal mechanically analysis in metal forming processes. In Pittman Wood Alexander Zienkiewicz, editor, *Numerical Methods in Industrial Forming Processes*, pages 425–434, (1982).

[9] P. Wriggers, C. Miehe, M. Kleiber, and J.C. Simo. On the coupled thermo-mechanical treatment of necking problems via FEM. In D.R.J. Owen, E. Hinton, and E. Oñate, editors, *International Conference on Computational Plasticity (COMPLAS2)*, pages 527–542, Barcelona, Spain, (1989). Pineridge Press.

[10] P. Perzyna. Fundamental problems in visco-plasticity. In G. Kuerti, editor, *Advances in Applied Mechanics*, volume 9, pages 243–377. Academic Press, (1966).

[11] P. Perzyna. Thermodynamic theory of plasticity. In Chia-Shun Yih, editor, *Advances in Applied Mechanics*, volume 11, pages 313–355. Academic Press, (1971).

[12] F. Armero and J.C. Simo. A new unconditionnaly stable fractionnal step method for non-linear coupled thermomechanical problem. *International Journal of Numerical Methods in Engineering*, **35**, 737–766 (1992).

[13] J.C. Simo and T.J.R Hughes. General return mapping algorithms for rate-independent plasticity. In *Constitutive Laws for Engineering materials : Theory and Applications*. Elsevier Science Publishing Co, (1987).

[14] J.P. Ponthot. Unified stress update algorithms for the numerical simulation of large deformation elasto-plastic and elasto-viscoplastic processes. *International Journal of Plasticity*, **18**, 91–126 (2002).

[15] J.P. Ponthot. *Traitement unifié de la Mécanique des Milieux Continus solides en grandes transformations par la méthode des éléments finis*. PhD thesis, University of Liège, Belgium, Liège, (1995).

[16] D. Graillet. *Modélisation tridimensionelle du contact entre structures à parois minces dans les phénomènes d'impacts et de mise en forme*. PhD thesis, University of Liège, Belgium, (In preparation).

[17] P. Wriggers and C. Miehe. Contact constraints within coupled thermomechanical analysis – a finite element model. *Computer Methods in Applied Mechanics and Engineering*, **113**, 301–319 (1994).

[18] C. Agelet de Saracibar. Numerical analysis of coupled thermomechanical frictional contact problems. computation model and applications. *Archives of Computational Methods in Engineering*, **5**(3), 243–301 (1998).

[19] P. Wriggers and C. Miehe. On the treatment of contact constraints within coupled thermomechanical analysis. In D.Besdo and E.Stein, editors, *Finite inelastic deformations - Theory and applications*, IUTAM Symposium, pages 333–347. Springer-Verlag, (1991).

[20] Beltran and Goicolea. Large strain plastic collapse : A comparison of explicit and implicit solutions. In D.R.J. Owen, E. Hinton, and E. Oñate, editors, *International Conference on Computational Plasticity (COMPLAS2)*, pages 1125–1136, Barcelona, Spain, (1989). Pineridge Press.

[21] C. Garcia Garino. *Un modelo numerico para el analysis de solidos elastoplasticos sometidos a grandes deformaciones*. PhD thesis, Universitat Politecnica de Catalunya - U.P.C.,

Barcelona, Spain, Spain, (1993).

[22] M.L. Wilkins. Calculation of elastoplastic flows. In B. Alder, editor, *Methods in Computational Physic*, volume 3, pages 211–263. Academic Press, (1964).